Array–enhanced coherence resonance and forced dynamics in coupled FitzHugh–Nagumo neurons with noise

Yuji Shinohara[1], Takashi Kanamaru[2], Hideyuki Suzuki[1], Takehiko Horita[1], and Kazuyuki Aihara[1,3]

[1]*Department of Mathematical Engineering and Information Physics, Graduate School of Engineering, The University of Tokyo, Hongo 7–3–1, Bunkyo-ku, Tokyo 113–8656, Japan*

[2]*Department of Electrical and Electronic Engineering, Tokyo University of Agriculture and Technology, Tokyo 184–8588, Japan,*

[3]*CREST, Japan Science and Technology Corporation (JST), 4–1–8 Hon-cho, Kawaguchi, Saitama 332–0012, Japan.*

(January 21, 2002)

Abstract

Nonlinear dynamics of coupled FitzHugh–Nagumo neurons subject to independent noise is analysed. A kind of self–sustained global oscillation with almost synchronous firing is generated by array–enhanced coherence resonance. Further, forced dynamics of the self–sustained global oscillation stimulated by sinusoidal input is analysed and classified to synchronized, quasi–periodic and chaotic responses just like forced oscillations in nerve membranes observed by *in vitro* experiments with squid giant axons. Possible physiological importance of such forced oscillations is also discussed.

PACS numbers: 87.10.+e, 05.45.-a, 07.05.Mh

I. INTRODUCTION

Neurons are fundamental elements constituting the biological brain. Information processing in the brain is believed to be supported by nonlinear dynamics of such neurons [1]. The nonlinear dynamics of neurons has been studied both experimentally and theoretically as a main topic in neuroscience [1,2]. In particular, squid giant axons and the mathematical model of the Hodgkin–Huxley equations have been greatly contributing to such research on nonlinear neurodynamics [3].

Well–controlled *in vitro* experiments with squid giant axons and corresponding theoretical analysis with the Hodgkin–Huxley equations have clarified existence of rich nonlinear phenomena in nerve membranes like a self–sustained oscillation with repetitive firing of action potentials and the Hopf bifurcation [4–6]. Moreover, as a simple case of interaction among such neural oscillators, forced oscillations of a self–sustained neural oscillator stimulated by periodic input such as sinusoidal and pulse–train currents have been intensively analysed and classified as synchronized, quasi–periodic, and chaotic oscillations [7–9]. Figures 1 (a), (b) and (c) show examples of a self–sustained oscillation with repetitive firing of action potentials, a 1/1–synchronized oscillation where one action potential is generated during each period of a sinusoidal force periodically, and a chaotic oscillation in squid giant axons. Here, the forced oscillations of Figs. 1 (b) and (c) are observed by stimulating a self–sustained oscillator of Fig. 1 (a) with a sinusoidal current which amplitude and frequency are changed as the bifurcation parameters [7–9]. In particular, existence of chaotic oscillations in squid giant axons like one of Fig. 1 (c) has been confirmed by examining the geometric structure of reconstructed attractors [10] as well as by calculating the indices of chaos such as the Lyapunov exponent [11] and deterministic predictability [12,13]. Further, neural oscillations have been also payed much attention as possible mechanism of functions in the brain like binding distributed pieces of information, although careful discussion on e.g. relation between synchrony and oscillations are indispensable [14].

When we consider nonlinear oscillations as neuronal correlates which actually play func-

tional roles in the brain, there exist two problems that should be carefully examined. Namely, (1) realization of neural oscillators by cortical neurons which dynamics is excitable rather than oscillatory and (2) effects of ubiquitous background noise to cortical neurons that operate in such a noisy environment.

Effects of noise on nonlinear dynamics like noise-induced order [15] and stochastic resonance [16] have been one of important topics in nonlinear science. Among these studies, coherence resonance (CR) and similar dynamics [17–27] are closely related to the two problems raised above. In particular, array–enhanced coherence resonance provides a possible mechanism that coupled excitable neurons subject to independent external noise operate like synchronized self–sustained oscillators generating almost regular firing of action potentials [26,27]. Moreover, interesting nonlinear phenomena such as synchronization of interacting coherence resonance oscillators [28] and global forced activities of coupled noisy excitable systems [29] have been also analysed.

In this paper, time series data of interspike intervals in coupled noisy excitable systems of the FitzHugh–Nagumo neurons [30,31] are analysed with nonlinear time series analysis which had been effective to elucidate nonlinear dynamics of squid giant axons directly from electrophysiological data [12,13].

II. ARRAY–ENHANCED COHERENCE RESONANCE IN COUPLED FITZHUGH-NAGUMO NEURONS

Based on the models in Refs. [20,25,27], coupled FitzHugh-Nagumo neurons in an $M \times N$ lattice is represented as follows :

$$\epsilon \dot{x}_{ij} = x_{ij} - \frac{x_{ij}^3}{3} - y_{ij} + \xi_{ij}(t) + g(x_{i+1,j} + x_{i-1,j} + x_{i,j+1} + x_{i,j-1} - 4x_{ij}), \quad (1)$$

$$\dot{y}_{ij} = x_{ij} + a \quad (2)$$

$$(i = 1, 2, \cdots, M,\ j = 1, 2, \cdots, N),$$

where ϵ, g and a are parameters and the periodic boundary condition such that $x_{M+1,j} = x_{1,j}$, $x_{-1,j} = x_{M,j}$, $x_{i,N+1} = x_{i,1}$, and $x_{i,-1} = x_{i,N}$ is employed. We set $\epsilon = 0.01$ and $a = 1.05$ to keep every neuron excitable so that the resting state is asymptotically stable if without any external inputs. The noise terms $\xi_{ij}(t)$ are independent Gaussian white noise with intensity D, i.e., $\langle \xi_{ij}(t)\xi_{kl}(t')\rangle = 2D\delta_{ik}\delta_{jl}\delta(t-t')$. The coupling among the elements is local and diffusive with strength g. Different from the neuron models in previous studies on coherence resonance (CR) [20,23,27], the noise terms are incorporated in eq. (1) rather than eq. (2) to explore effects of background current noise to the variable x which corresponds to the membrane potential of a neuron.

Let the sequence $t_0^{(ij)} < t_1^{(ij)} < t_2^{(ij)} < \cdots < t_{K_{ij}}^{(ij)}$ denote the series of firing times of x_{ij}. From the sequence of $\{t_k^{(ij)}\}$, the interspike intervals (ISI) are defined as $T_k^{(ij)} = t_k^{(ij)} - t_{k-1}^{(ij)}$ $(k = 1, 2, \cdots, K_{ij})$. To characterize the coherence of the output spike train, the coherence measure R is defined as follows [20,27]:

$$R = \frac{\langle T_k^{(ij)} \rangle}{\sqrt{\langle (T_k^{(ij)})^2 \rangle - \langle T_k^{(ij)} \rangle^2}}, \tag{3}$$

where

$$\langle (T_k^{(ij)})^n \rangle = \frac{\sum_{i=1}^{M} \sum_{j=1}^{N} \sum_{k=1}^{K_{ij}} (T_k^{(ij)})^n}{\sum_{i=1}^{M} \sum_{j=1}^{N} K_{ij}}. \tag{4}$$

In short, R is the ratio of the average and the standard deviation of the interspike intervals and is a kind of signal–to–noise ratio in the meaning that periodicity with repetitive firing at fixed intervals is a signal. It should be noted that R is the reciprocal of the coefficient of variation in a point process that is widely used in the field of neuroscience [1,32,33].

We have numerically calculated R as a function of g and D for the two-dimensional square lattice with $M = N$ and the one-dimensional lattice with $M = 1$. The features of the dependence of R on g and D are almost the same as those reported in Ref. [27] where the setup of the system is different from that of the present paper in the following meaning; the slow variable y is perturbed by the noise, the parameter a of each element is randomly distributed over an interval, and the lattice is one-dimensional [27]. The system of eqs. (1)

and (2) exhibits *array-enhanced CR* [27], i.e., there exists an optimal pair of noise intensity and coupling strength, both in the two-dimensional square lattice and in the one-dimensional lattice. By the numerical experiment, as shown in Fig. 2, we have found that the maximum value R^* of R at the optimal D and g increases with the system size and saturates around $\bar{R} \sim 40$ and $\bar{R} \sim 26$ for the two-dimensional and one-dimensional lattices, respectively. It is also observed that the optimal noise intensity and the optimal coupling strength converge to constants, which is contrasted with the case of array-enhanced stochastic resonance where the optimal noise intensity and the optimal coupling strength satisfy scaling relations with the system size [34]. The saturation of the value of R with increasing the system size is phenomenologically understood by observing a sequence of activity pattern of a large system at the optimal pair of noise intensity and coupling strength. As shown in Fig. 3, several spots of firing appear first, then they grow into global firing; thus, for each element, there is an effective size of system which is relevant to the firing of the element. As a result, the degree of overall synchronization of firing becomes worse with increase of the system size [25]. By assuming the existence of the effective system size, it is concluded that the maximum value R^* of R does not depend on the system size for systems larger than the effective system size. A detailed analysis concerning the existence of the effective system size is left as a future work.

We can conclude that the two-dimensional lattice can achieve more coherence than the one-dimensional one. Roughly speaking, this enhancement of CR by the increase of the dimension of the lattice is considered to be due to the fact that firing of one element can propagate more easily to the other elements and synchronization of the elements takes place more easily with a moderate strength of the coupling.

Figure 4 shows a typical time series of x_{11} with a high value of R. Despite the randomness of the noise input, it shows nearly periodic oscillation with repetitive firing of action potentials. This coherence resonance oscillation results from the collective motion of the diffusively coupled neurons subject to independent noise. In the next section, we perturb this noise-induced coherent oscillation by periodic sinusoidal input, to consider effects of

interaction between the two oscillatory modes, namely a self–sustained oscillation and an external periodic force.

III. FORCED DYNAMICS OF COHERENCE RESONANCE OSCILLATORS

Under the condition that g and D are set so that R is nearly maximized, let us periodically perturb the system with sinusoidal input [7–9,29]. Then, eq. (1) is modified to include the periodic forcing term as follows:

$$\epsilon\dot{x}_{ij} = x_{ij} - \frac{x_{ij}^3}{3} - y_{ij} + \xi_{ij}(t) + A\sin\left(\frac{2\pi t}{B}\right) + g(x_{i+1,j} + x_{i-1,j} + x_{i,j+1} + x_{i,j-1} - 4x_{ij}). \tag{5}$$

In order to observe interaction between the two oscillatory modes, the amplitude A of the periodic forcing is set at a relatively large value $A = 0.1$; when $D = 0$ and $M = N = 1$, namely in the case of a single neuron, this strength is suprathreshold for $0.2 \leq B \leq 7.1$ and subthreshold for $B \geq 7.2$. The system size is fixed at $M = N = 10$ and the noise intensity and the strength of coupling are determined as $D = 4.0 \times 10^{-5}$ and $g = 0.06$ so that R attains its almost maximum value ~ 38 at the present system size. Note that $R \sim 38$ is close to the limiting value $\bar{R} \sim 40$ in the large system size limit and in this sense the system size $M = N = 10$ is considered to be large enough. In the following, the sequence $\{T_1, T_2, \cdots, T_K\}$ of interspike intervals of x_{11} is analysed.

In Fig. 5, the firing rate $\rho \equiv BK/(\sum_{i=1}^{K} T_i)$, i.e., the average frequency of firing during one period of external forcing, is plotted against the period B of the external force. There are plateaus with simple rational values of the firing rates, which commonly appear in deterministic two-frequency systems and indicate synchronized oscillations [35]. As in the deterministic systems, between two adjacent plateau regions competition between the two oscillatory modes is expected to generate non-trivial motion. In the deterministic systems, the typical non-trivial motion is a chaotic oscillation [7–9,35], while quasi-periodic motion is also typical but trivial.

The left column of Fig. 6 shows plots of T_{i+1} against T_i for several values of B implying that the system is well reconstructed on the T_i–T_{i+1} plane [36]. At $B = 3.3$ corresponding to the plateau at the firing rate $\rho = 1$, the points on the T_i–T_{i+1} plane form one cluster showing a nearly 1/1–synchronized oscillation. Similar analysis confirms that each plateau of the firing rates in Fig. 5 represents a phase-locked synchronized motion. Since the system is subject to random noise, it should be noted that there is a non-zero probability that the response is accidentally unlocked, i.e., the point deviates temporarily away from clusters corresponding to a periodic point on the T_i–T_{i+1} plane, in the observation over a long time.

At $B = 2.5$, 5.0, and 10.0, the phase-unlocked motions are observed; there appear nonlocalized points on the T_i–T_{i+1} plane and the return plots of phases $\varphi_i = 2\pi t_i^{(11)}/B \pmod{2\pi}$. Our interest here is whether the motions have deterministic instability or not, i.e., whether the system inherently generates complex motions according to a kind of determinism or not. If the answer is affirmative, then the motions are considered to be a counterpart of chaotic oscillations.

In order to characterize the observed interspike interval data from the viewpoint of determinism, let us explore the normalized prediction error (NPE) with the nearest-neighbor method of prediction [36,37]. With the reconstructing dimension m and delay coordinate vectors of interspike intervals $V_j = (T_{j-m+1}, \cdots, T_j)$, the dynamical behavior is reconstructed in $\boldsymbol{R}^m$. Here we take $m = 3$ which seems to be appropriate as shown in Fig. 6. Let L be the number of state points in the reconstructed phase space $\boldsymbol{R}^m$ and, for a fixed j_0, choose $l = \beta L (\beta < 1)$ points that are nearest to the point V_{j_0} in $\boldsymbol{R}^m$ and denote them by $V_{j_k} = (T_{j_k-m+1}, \cdots, T_{j_k})$ $(k = 1, 2, \cdots, l)$. With $\{V_{j_k}\}$ $(k = 1, 2, \cdots, l)$, a predictor of T_{j_0+h} for h steps ahead is constructed by the following average [36,37]:

$$p_{j_0}(h) = \frac{1}{l} \sum_{k=1}^{l} T_{j_k+h}. \tag{6}$$

The normalized prediction error (NPE) is defined by

$$\mathrm{NPE} = \frac{\langle (p_{j_0}(h) - T_{j_0+h})^2 \rangle^{\frac{1}{2}}}{\langle (\langle T_{j_0} \rangle - T_{j_0+h})^2 \rangle^{\frac{1}{2}}}, \tag{7}$$

where $\langle\cdot\rangle$ stands for the average with respect to j_0 over the observed sequence. If the NPE is much less than 1, it can be said that the deterministic prediction fits well to the time series. The small NPE indicates the existence of deterministic structure behind the time series data, because this algorithm is based on the assumption that the dynamical structure of a finite-dimensional deterministic system can be well reconstructed by the delay coordinates of interspike interval data [36]. In order to confirm the deterministic property, the values of NPE should be compared with those of NPE for a set of surrogate data [38]. The surrogate data are new time series generated from the original time series under some null hypothesis so that the new time series preserves some statistical properties of the original data. Here, we use three kinds of surrogation, namely, random shuffled (RS), Fourier shuffled (FS), and amplitude adjusted Fourier transformed (AAFT) surrogate data which respectively correspond to the null hypotheses of independent and identically distributed random process, a linear stochastic process, and a linear stochastic process observed through a monotonic nonlinear function [37,38].

Figure 7 shows NPE with $m = 3$, $L = 3000$, and $\beta = 0.01$ as a function of prediction steps h for each value of B used in Fig. 6. For the phase-locked motion with the firing rate 1 in Fig. 6 (a), each NPE has a value close to 1. This is due to the fact that for the synchronized motion the interspike intervals T_i slightly fluctuate around a constant value with small and almost independent fluctuation.

In the case with $B = 10.0$ where an almost closed curve and a monotonous and invertible circle map are observed in the T_i–T_{i+1} plane and the return plots of phases in Fig. 6 (b), respectively, the NPE is small compared with those of the surrogate data and almost constant for $1 \leq h \leq 9$ as shown in Fig. 7 (b), suggesting that the motion corresponds to a quasi-periodic oscillation in deterministic systems. In the cases with $B = 2.5$ and 5.0, the NPEs are relatively small at $h = 1$ and monotonically increase with increasing h to values close to 1. The motions are predictable for $h = 1$ and the deterministic predictability is gradually lost with the increase of the prediction step h. This implies that the motion has deterministic instability. From the dependence of NPE on h, the system with $B = 5.0$ is considered to

have stronger instability than the system with $B = 2.5$.

Figures 6 and 7 enable us to classify the observed responses into three kinds of motions, namely the synchronized and phase-locked motion, the phase-unlocked motion without deterministic instability, and the phase-unlocked motion with deterministic instability. Thus, interaction between two kinds of oscillatory modes, one sustained by array–enhanced CR with the noise and the other of external periodic forcing, produces a motion with deterministic instability, which is non-trivial in the following senses: this is neither the case where an underlying chaotic motion is perturbed by noise nor the case where noise is just nonlinearly amplified by the dynamics. Indeed at $D = 0$ only a synchronized motion with the external forcing is observed for $B \leq 7.1$ and no firing is observed for $B \geq 7.2$. This non-trivial motion may be called CR–sustained deterministic chaos where almost synchronous firing is generated repetitively and chaotically from forced CR oscillators.

IV. CONCLUSION

Coherence resonance in coupled FitzHugh-Nagumo models in lattices is examined and the array-enhanced coherence resonance is observed. It is found that higher coherence is achieved in the two-dimensional lattice compared with the one-dimensional one; the maximum of R as a function of the noise intensity D and the strength g of coupling has larger values in the two-dimensional lattice than in the one-dimensional one. The periodic perturbation of the coherence resonance oscillation with high R generates three kinds of motions, namely, the phase-locked synchronized motion, the phase-unlocked motion without deterministic instability, and the phase-unlocked motion with deterministic instability, which correspond to a synchronized oscillation, a quasi–periodic oscillation, and a chaotic oscillation in deterministic systems [7,9,35], respectively. It is remarked that the phase-unlocked motion with deterministic instability is non-trivial and a counterpart of deterministic chaos.

In conclusion, an assembly of the excitable neuron models subject to independent noise cooperatively generates a highly coherent oscillation with repetitive and almost synchronous

firing of action potentials by array–enhanced coherence resonance [27]. Periodic forcing, which can be realized by interaction between such two assemblies with array–enhanced coherence resonance, can generate such rich forced responses as synchronous, quasi–periodic, and chaotic ones, just like forced oscillations in nerve membranes observed by well–controlled *in vitro* experiments with squid giant axons [7–9]. This result implies that neural oscillators which existence has been assumed in theoretical models of many dynamical neural networks and physiologically confirmed by *in vitro* experiments as shown in Fig. 1, are not necessarily specific to such theoretical and experimentally well-controlled situations but biologically plausible because such oscillators can be self–organized by coupled neurons, which dynamics is excitable rather than oscillatory and subject to background noise similarly to cortical neurons in the biological brain.

REFERENCES

[1] C. Koch, *Biophysics of Computation : Information Processing in Single Neurons* (Oxford Univ. Press, Oxford, 1999).

[2] T. McKenna, J. Davis, and S.F. Zornetzer (Eds.), *Single Neuron Computation* (Academic Press, Boston, 1992).

[3] A.L. Hodgkin and A.F. Huxley, J. Physiol. (London) **117**, 500 (1952).

[4] A.F. Huxley, Ann. N.Y. Acad. Sci. **81**, 221 (1959).

[5] B. Hassard, J. Theor. Biol. **71**, 401 (1978).

[6] K. Aihara and G. Matsumoto, J. Theor. Biol. **95**, 697 (1982).

[7] K. Aihara and G. Matsumoto, in *Chaos*, edited by A.V. Holden (Manchester Univ. Press, Manchester, and Princeton Univ. Press, Princeton, 1986), p. 257.

[8] G. Matsumoto, K. Aihara, M. Ichikawa, and A. Tasaki, J. Theor. Neurobiol. **3**, 1 (1984).

[9] K. Aihara, G. Matsumoto, and Y. Ikegaya, J. Theor. Biol. **109**, 249 (1984).

[10] K. Aihara, T. Numagiri, G. Matsumoto, and M. Kotani, Phys. Lett. A **116**, 313 (1986).

[11] R.M. Everson, in *Chaos in Biological Systems*, edited by H. Degn, A.V. Holden, and L.F. Olsen (Plenum Press, N.Y., 1987), p. 133.

[12] A. Mees, K. Aihara, M. Adachi, K. Judd, T. Ikeguchi, and G. Matsumoto, Phys. Lett. A **169**, 41 (1992).

[13] K. Aihara, T. Ikeguchi, and G. Matsumoto, Int. J. Chaos Theory and Applications **3**, 5 (1998).

[14] W. Singer, in *Models of Neural Networks II*, edited by E. Domany, J.L. van Hemmen, and K. Schulten (Springer–Verlag, N.Y., 1994), p. 141.

[15] K. Matsumoto and I. Tsuda, J. Stat. Phys. **31**, 757 (1983).

[16] e.g. L. Gammaitoni, P. Hänggi, P. Jung, and F. Marchesoni, Rev. Mod. Phys. **70**, 223 (1998).

[17] H. Gang, T. Ditzinger, C.Z. Ning, and H. Haken, Phys. Rev. Lett. **71**, 807 (1993).

[18] C. Kurrer and K. Schulten, Phys. Rev. E **51**, 6213 (1995).

[19] W.J. Rappel and A. Karma, Phys. Rev. Lett. **77**, 3256 (1996).

[20] A.S. Pikovsky and J. Kurths, Phys. Rev. Lett. **78**, 775 (1997).

[21] A. Longtin, Phys. Rev. E **55**, 868 (1997).

[22] S.-G. Lee, A. Neiman, and S. Kim, Phys. Rev. E **57**, 3292 (1998).

[23] B. Lindner and L. Schimansky -Geier, Phys. Rev. E **60**, 7270 (1999).

[24] H. Hempel, L. Schimansky-Geier, and J. García-Ojalvo, Phys. Rev. Lett. **82**, 3713 (1999).

[25] A. Neiman, L. Schimansky-Geier, A. Cornell-Bell, and F. Moss, Phys. Rev. Lett. **83**, 4896 (1999).

[26] Y. Wang, D.T.W. Chik, and Z.D. Wang, Phys. Rev. E **61**, 740 (2000).

[27] B. Hu and C. Zhou, Phys. Rev. E **61**, R1001 (2000); C. Zhou, J. Kurths, and B. Hu, Phys. Rev. Lett. **87**, 098101 (2001).

[28] S.K. Han, T.G. Yim, D.E. Postnov, and O.V. Sosnovtseva, Phys. Rev. Lett. **83**, 1771 (1999).

[29] S. Tanabe, T. Shimokawa, S. Sato, and K. Pakdaman, Phys. Rev. E **60**, 2182 (1999).

[30] R. FitzHugh, in *Biological Engineering, 1*, edited by H.P. Schwan (McGraw–Hill, N.Y., 1969), p. 1.

[31] J. Nagumo, S. Arimoto, and S. Yoshizawa, in *Proc. IRE, 1962*, Vol. 50, p. 2061.

[32] W.R. Softkey and C. Koch, J. Neurosci. **13**, 334 (1993).

[33] F. Gabbiani and C. Koch, in *Methods in Neural Modeling*, edited by C. Koch and I. Segev (MIT Press, Cambridge, 1998), p. 313.

[34] J.F. Lindner, B.K. Meadows, W.L. Ditto, M.E. Inchiosa, and A.R. Bulsara, Phys. Rev. E **53**, 2081 (1996).

[35] e.g. P. Bergé, Y. Pomeau, and C. Vidal, *Oder within chaos* (J. Wiely & Sons, N.Y., 1986); E. Ott, *Chaos in dynamical systems* (Cambridge Univ. Press, Cambridge, 1993).

[36] T. Sauer, Phys. Rev. Lett. **72**, 3811 (1994).

[37] H. Suzuki, K. Aihara, J. Murakami, and T. Shimozawa, Biol. Cybern. **82**, 305 (2000).

[38] J. Theiler, S. Eubank, A. Longtin, B. Galdrikan, and J. D. Farmer, Physica D **58**, 77 (1992).

FIGURES

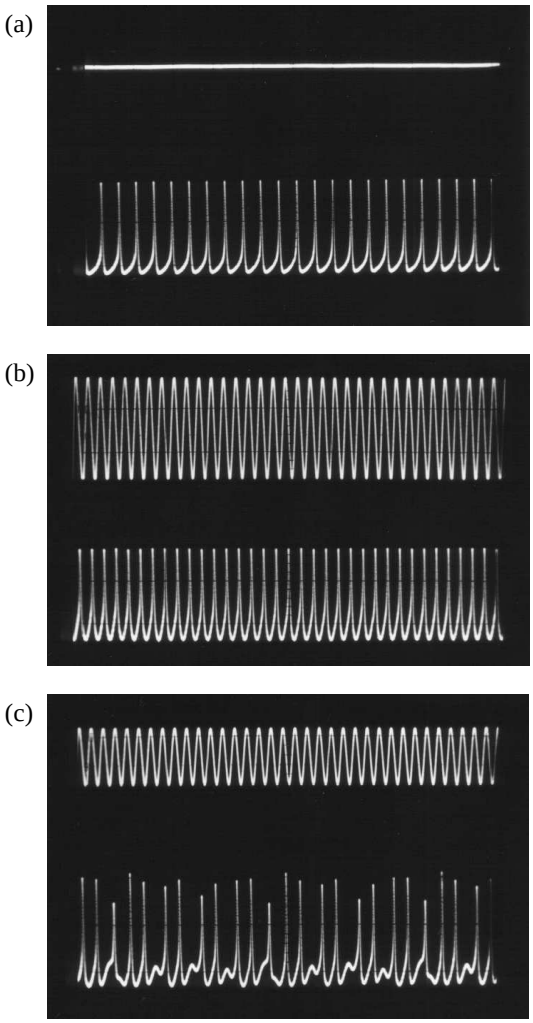

FIG. 1. Examples of electrophysiological results with squid giant axons. (a) a self-sustained oscillation with repetitive firing of action potentials, (b) a 1/1–synchronized forced oscillation, and (c) a chaotic forced oscillation. In each figure, the upper and lower waveforms show the stimulating current and the membrane potential, respectively. Giant axon of squid (*Doryteuthis bleekeri*) were used in the experiment. The self–sustained oscillation in (a) was induced by bating the axon in mixture of natural sea water and 550mM NaCl [6]. The forced oscillations in (b) and (c) were produced by stimulating the self–sustained neural oscillator with sinusoidal currents through an internal platinized platinum wire electrode [8].

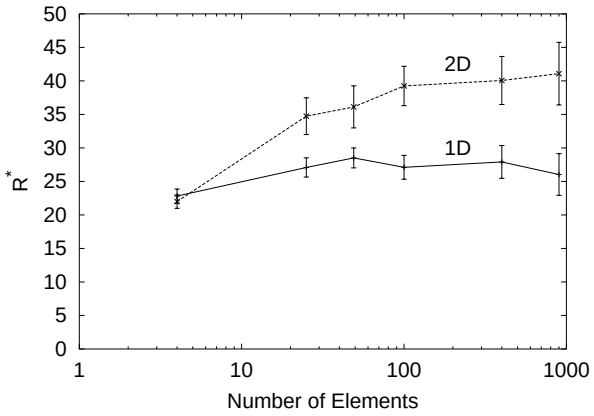

FIG. 2. System size dependence of the maximum R^* of R for the one-dimensional and two-dimensional lattices. Saturation of the growth of R^* is observed in large system sizes.

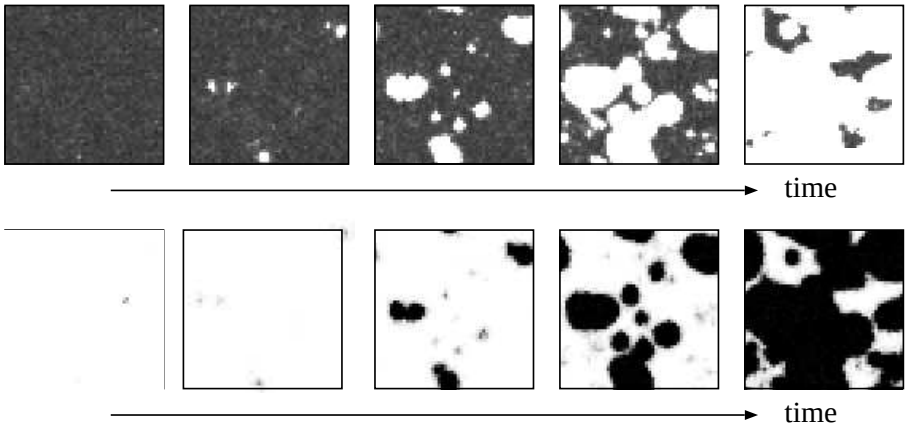

FIG. 3. A sequence of activity patters $\{x_{ij}\}$ at time intervals of 0.1 around synchronous firing for the two-dimensional lattice with $N = M = 50$, $D = 6 \times 10^{-5}$, and $g = 0.08$. The whiter point corresponds to high values of x showing firing.

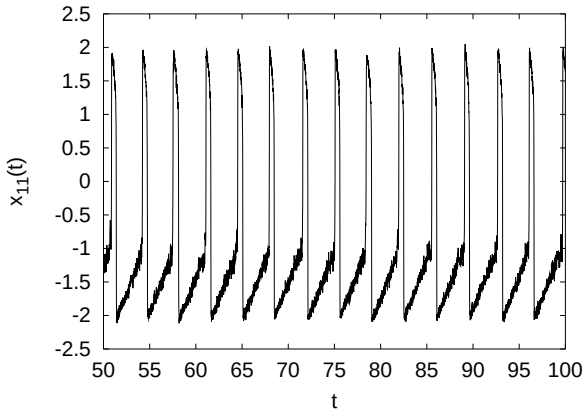

FIG. 4. A time-series of x_{11} with $N = M = 10$, $g = 0.06$, and $D = 4.0 \times 10^{-5}$ in a state of a coherence resonance oscillation sustained by noise and coupling.

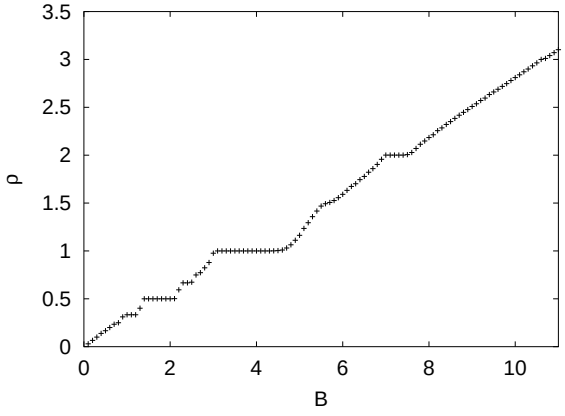

FIG. 5. The relation between the average firing rate ρ and the period B of the external forcing.

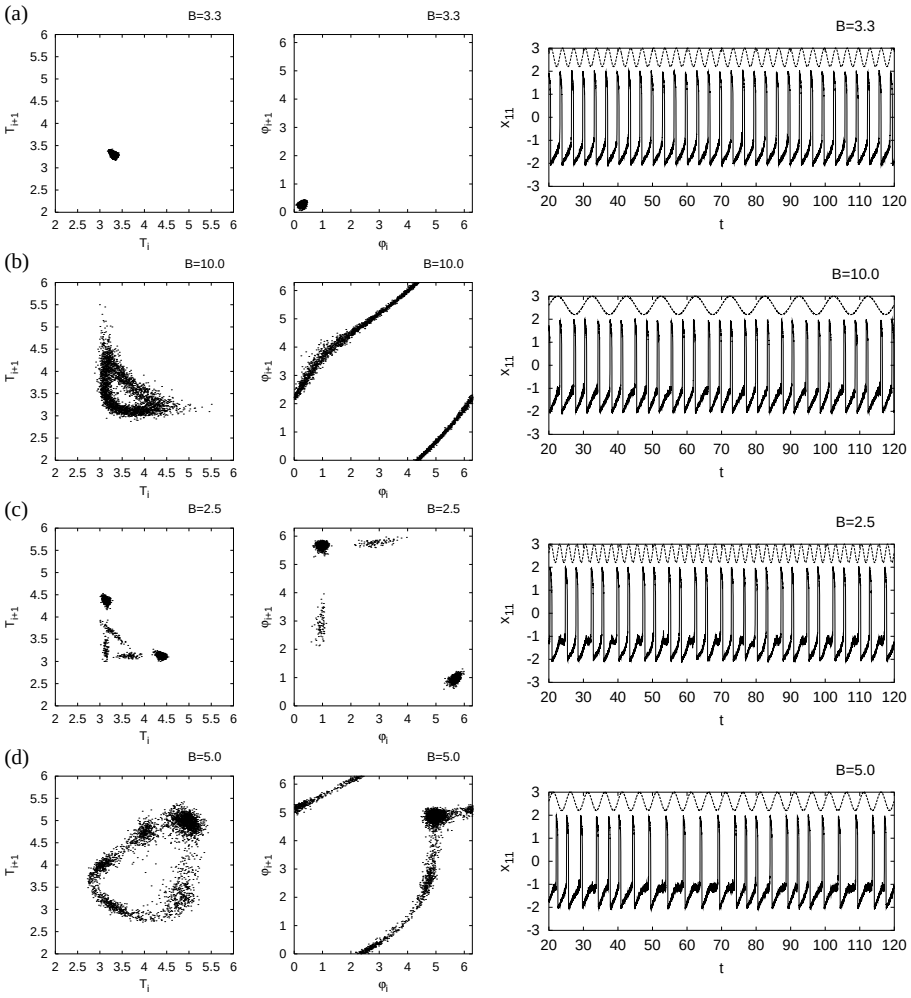

FIG. 6. Two–dimensional reconstruction with T_i and T_{i+1} (left), return plots on phases (middle), and waveforms (right) of the variable x (lower) and the stimulation (upper) for B = (a) 3.3, (b) 10.0, (c) 2.5, and (d) 5.0. Here, the phases of the middle column are defined as follows : $\varphi_i \equiv 2\pi t_i^{(11)}/B \pmod{2\pi}$.

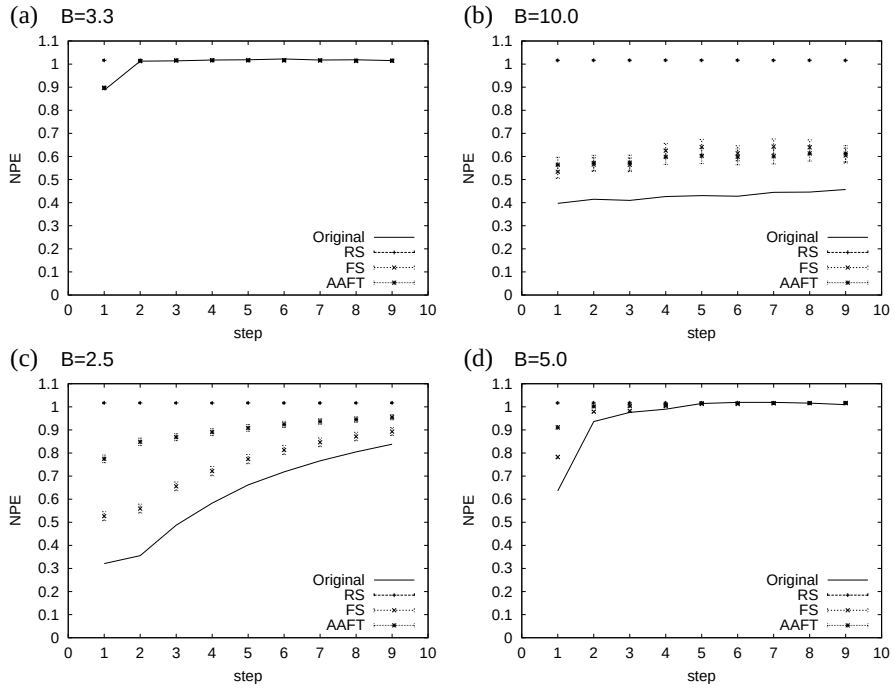

FIG. 7. The relation between NPE and prediction steps h for B = (a) 3.3, (b) 10.0, (c) 2.5, and (d) 5.0. The solid lines show NPE of the original data.